

# Slender metal web stability analysis: Impact of initial imperfection on the mode of buckling

*Martin Psotný*<sup>1,\*</sup>

<sup>1</sup>Slovak University of Technology, Faculty of Civil Engineering, Department of Structural Mechanics, Radlinskeho 11, 810 05 Bratislava, Slovak Republic

**Abstract.** The post buckling of a rectangular slender web in compression has been analyzed. Shapes of a buckling area obtained from the nonlinear analysis have been compared with buckling modes from the linearized problem for various aspect ratios. Effects of initial shape imperfections upon the analysis have been investigated using nonlinear approach. To trace the complete nonlinear equilibrium curves, specialized code based on FEM was created. The Newton-Raphson iteration algorithm was used, load versus displacement control was changed during the process of calculation. Obtained results were verified using Ansys system, in this case arc-length method was activated for overcoming critical points.

## 1 Introduction

Slender web of rectangular shape has been the simplest, easy to made shape, therefore has been widely used in engineering. Such webs occur as parts of marine, automotive and aircraft structures in mechanical engineering, as parts (stiffened webs) of girders in civil engineering. Such webs subjected to the edge compressive loads are susceptible to the buckling due to dominant compressive membrane force within the structure. Stored strain energy can be suddenly released and converted into kinetic energy with subsequent large displacements and very often with resultant collapse of the structure.

Analysing stability of the slender web, it has not been usually enough to determine the elastic critical load solving eigenvalue buckling analysis, i.e. the load, under which the perfect web starts buckling. It is essential to include as many initial imperfections of real web into the solution as possible and determine limit load level more accurately. The geometrically nonlinear theory [1, 2] represents a basis for the reliable description of this problem.

## 2 Theoretical assumptions

A rectangular slender web with the dimensions  $a \times b$  and with the thickness  $t$  simply supported along all edges has been considered in Fig. 1. Web is subjected to the compressive edge load  $p$  in one direction and it is assumed that web buckles into  $m$

---

\* Corresponding author: [martin.psotny@stuba.sk](mailto:martin.psotny@stuba.sk)

sinusoidal half-waves in the direction of loading (and  $n$  sinusoidal half-waves in the perpendicular direction).

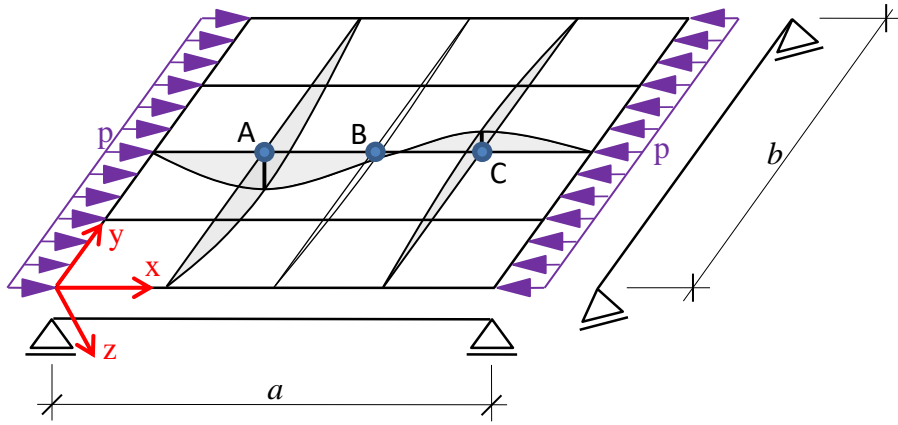


**Fig. 1.** Rectangular slender web subjected to edge load in one direction. Notations of the quantities.

### 2.1 Eigenbuckling - linearized stability analysis

Let us move to present linear stability solution first for slender webs with length/width ratios in general. In Fig. 2 we can see the well-known  $K$ - $\alpha$  curves (relationship between plate-buckling coefficient  $K$  ( $\sigma_{CR}/\sigma_{EU}$ ) and aspect ratio  $\alpha$  for different values  $m/n$  - number of halfwaves along  $a$ , along  $b$ ). It has been well-known diagram [3, 4], minimum value of  $\sigma_{CR}$  has not decreased under  $4\sigma_{EU}$  (thick line) and creates garlands. It is obvious, that critical stress for slender web with  $\alpha = 1$  buckling into mode 1-1 is the same as that for a web of  $\alpha = 2$  buckling into mode 2-1.

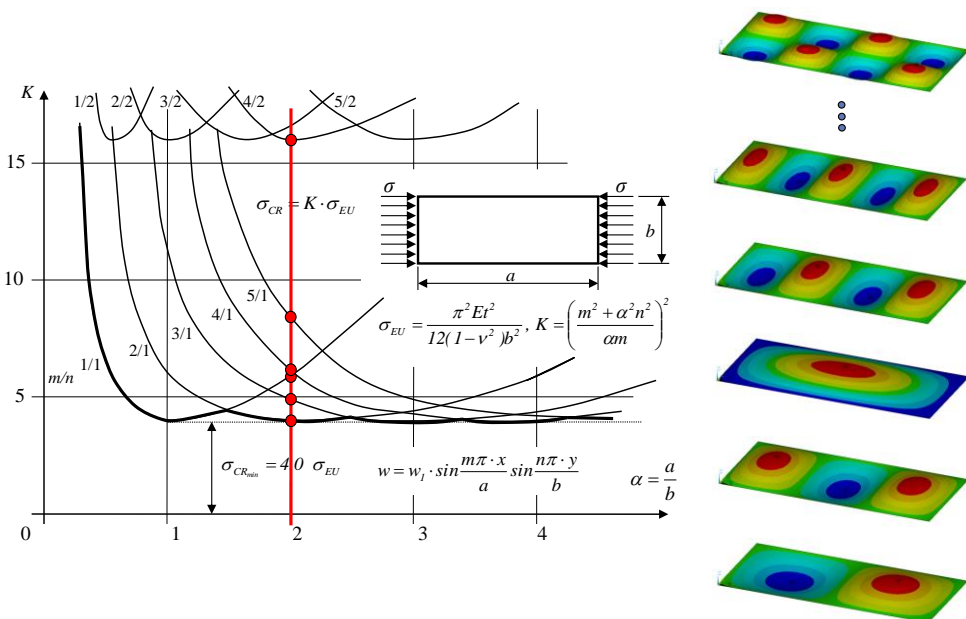


**Fig. 2.**  $K$ - $\alpha$  curves for different values  $m/n$ . Solution for  $\alpha = 2$  highlighted on the right.

This also means that the infinitely long web is also buckling in square waves and critical stress is also near  $4\sigma_{EU}$ .

Next part of the article has been focused on the slender web with  $\alpha = 2$ . Example of steel web with  $a = 240$  mm,  $b = 120$  mm and thickness  $t = 1$  mm has been assumed, modes of buckling of eigenvalue problem are plotted on the right of the figure, values of the corresponding critical loads have been in accordance with intersections of red vertical line and individual girlands in Fig. 2. Comparison with nonlinear solution follows.

### 2.2 Nonlinear stability analysis

The geometrically nonlinear theory represents a basis for the reliable description of the post-buckling behaviour of slender web. The result of the numerical solution represents a number of the load - versus displacement paths [5]. This result cannot be achieved directly, and the solution is based on a step by step incremental process that causes a deviation from the equilibrium nonlinear path. To correct this deviation, an iterative technique, Newton-Raphson method is used. Murray and Wilson [6] first presented idea of combining incremental and iterative methods for solving nonlinear problems in 1969.

In the case of a more complicated loading path, it is possible to utilize a calculation of controlled displacement increment. Displacement control procedure was first presented by Batoz and Dhatt [7] in 1979. In the case of snap-back, this option fails, but there are still some perspectives in the possibility to change the pivot parameter during the calculation [8, 9]. In this case the interactive approach and calculation check are requisite.

Using arc-length method to pass limit points on load-displacement paths introduced Riks in [10]. Crisfield incorporated mentioned problematic into computer codes in famous book [1]. Using the hitherto obtained knowledge and picking up work of Ravinger [5], author has presented results obtained as outputs of an own code for analysis of geometrically nonlinear tasks of perfect and imperfect slender webs [11, 12].

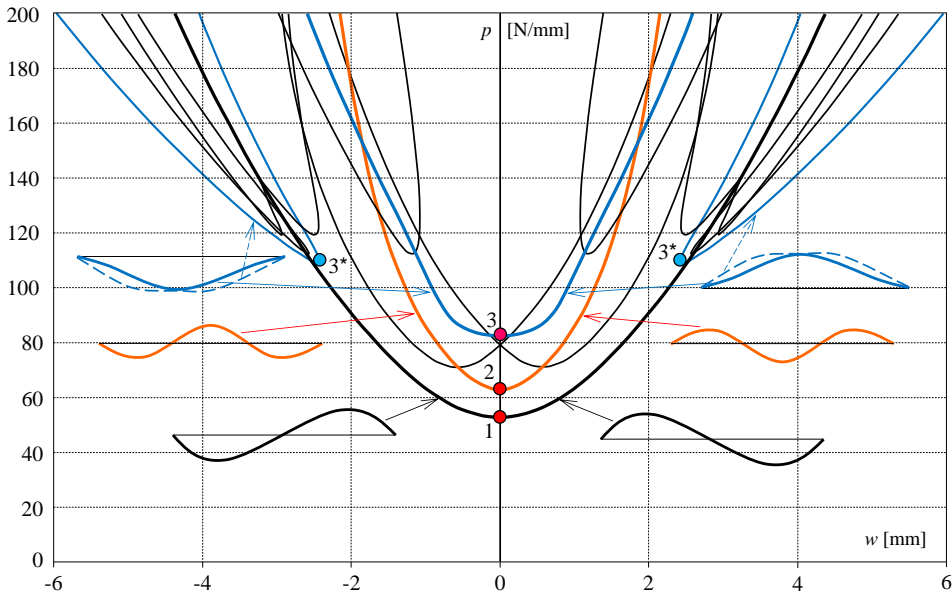
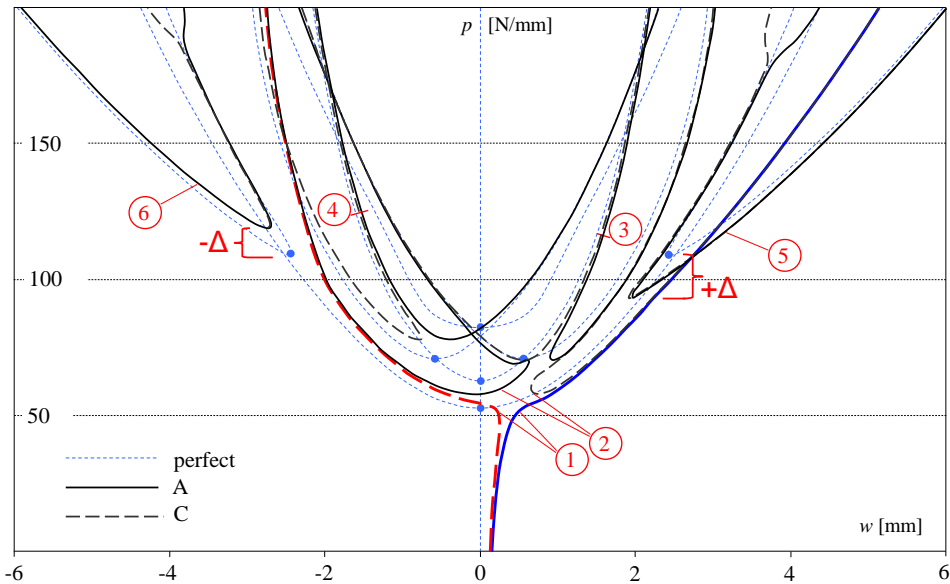


Fig. 3. Perfect slender web with aspect ratio  $\alpha = 2$ .

Let us move on to the results of nonlinear analysis of the slender web with  $\alpha = 2$  mentioned in the previous chapter. Interesting information points to the fact, that new load-displacement paths appear comparing to the web with  $\alpha = 1$  and solution has become less comprehensible. Due to this reason, in Fig. 3, solution of perfect web without initial geometrical imperfections has been presented first (due to the better description of buckling mode, out of plane nodal displacements in nodes denoted A and C have been taken as the reference values - see Fig. 1), however paths are not separated in the diagram. In case of perfect web, some paths are doubled, the others overlap due to the symmetry of solution. As expected, one can see that paths representing buckling in mode 2-1 emerge from the bifurcation point of the lowest load level (1). Load level in bifurcation point 2 (paths emerging from this bifurcation point represent buckling in mode 3-1) is also lower than the load level in bifurcation point 3 with paths representing buckling in basic mode 1-1. Also paths turning in limit points 3\* represent buckling in mode 1-1 (with higher corresponding load level). Other paths shown around bifurcation point 2 represent different forms of the transition between modes 2-1 and 3-1. Sections through the buckling area on mentioned equilibrium paths are also depicted in Fig. 3.

Nonlinear solution of slender web with initial geometrical imperfection similar to the mode 1-1 is presented in Fig. 4. Thick continuous lines denote the displacement in A, thick dashed lines refer to displacement in C. Solution of perfect web without initial imperfection is plotted by thin dashed lines on the background for comparison. We can see how individual paths of imperfect solution have been placed, when mode of buckling is similar to solution of perfect web and vice versa, when is significantly different. To simplify the Figure, only the paths being mentioned in the text above are plotted here.



**Fig. 4.** Web with initial imperfection  $w_0 = 0.2 \cdot \sin \frac{\pi \cdot x}{a} \sin \frac{\pi \cdot y}{b} + 0.01 \cdot \sin \frac{2\pi \cdot x}{a} \sin \frac{\pi \cdot y}{b}$ .

Web buckles in mode 1-1 on the prebuckling phase of fundamental path of solution (identical to the mode of initial imperfection). When the load reaches a value close to the load level in bifurcation point 1 of perfect web solution, curve representing displacement in C rapidly moves into negative values and postbuckling mode of the web is 2-1.

More details about the solution and quality analysis of the equilibrium paths have been mentioned in [11, 13].

### 3 Shape of initial imperfection and its influence of postbuckling

At the end of this paper let us pay attention to two slender webs with different aspect ratios. Material used in the analysis is an aluminium alloy 7020-T6 (Elastic Modulus 70 GPa, Poisson’s ratio 0.33, Shear Modulus 26 GPa, Tensile Strength, Yield >280 MPa 0.2% offset).

Slender web No. 1 parameters:  $a = 310$  mm,  $b = 220$  mm,  $t = 2$  mm,  $\alpha = 1.409$

Slender web No. 2 parameters:  $a = 352$  mm,  $b = 208$  mm,  $t = 2$  mm,  $\alpha = 1.692$

Why these two? From Fig. 2 it can be seen, that transition from mode  $m/n$  to mode  $m+1/n$  half-waves occurs when successive curves have equal values of  $K$ . Assuming transition from  $m = 1$  to  $m = 2$ , the intersection occurs at a value of  $\alpha = 1.41$ . This means that the perfectly flat web No. 1 will still buckle in shape 1-1, perfectly flat web No. 2 in shape 2-1. If the slender web is not initially flat, the situation may be different. Let us consider the initial shape imperfection in the form

$$w_0 = \alpha_1 \cdot \sin \frac{\pi \cdot x}{a} \sin \frac{\pi \cdot y}{b} + \alpha_2 \cdot \sin \frac{2\pi \cdot x}{a} \sin \frac{\pi \cdot y}{b} + \alpha_3 \cdot \sin \frac{3\pi \cdot x}{a} \sin \frac{\pi \cdot y}{b} \quad (1)$$

In next two Tables we can see how values of multipliers  $\alpha_1$ ,  $\alpha_2$  and  $\alpha_3$  affect the shape of the web in postbuckling. All presented results from nonlinear calculations were obtained using ANSYS system [14].

**Table 1.** Slender web No. 1,  $\alpha = 1.409$ .

model	$\alpha_1$ [mm]	$\alpha_2$ [mm]	$\alpha_3$ [mm]	postb. mode
1	0.5	0	0	1-1
2	0	0.5	0	2-1
3	0	0	0.5	3-1
4	0.5	0.5	0	2-1
5	0.5	0	0.5	1-1
6	0	0.5	0.5	2-1

**Table 2.** Slender web No. 2,  $\alpha = 1.692$ .

model	$\alpha_1$ [mm]	$\alpha_2$ [mm]	$\alpha_3$ [mm]	postb. mode
1	0.5	0	0	1-1
2	0	0.5	0	2-1
3	0	0	0.5	3-1
4	0.5	0.5	0	2-1
5	0.6	0.5	0	2-1
6	0.5	0	0.5	3-1
7	0	0.5	0.5	2-1
8	0.5	0.1	0.5	3-1
9	0.5	0.3	0.5	3-1
10	0.5	0.5	0.5	2-1

## 4 Conclusions

It can be seen that in the first case  $\alpha$  is very close to the intersection of the garlands for  $m = 1$  and  $m = 2$ . It follows that the postbuckling mode is either 1-1 or 2-1 (the only exception is the theoretical case - model 3). In the second case we can see the transition between  $m = 2$  and  $m = 3$  (except the theoretical case - model 1).

It is essential that presented solutions have been obtained by proper combining of load control and displacement control. Evidently, if we have an appropriate algorithm and enough time, it is not necessary to use more complex and complicated numerical techniques.

Presented results have been arranged due to the research supported by the Slovak Scientific Grant Agency, project No. 1/0453/20.

## References

1. M. A. Crisfield, *Non-Linear Finite Element Analysis of Solids and Structures* (Wiley&Sons, London, 1996)
2. F. Bloom, D. Coffin, *Handbook of Thin Plate Buckling and Postbuckling* (Chapman&Hall/CRC, Boca Raton, 2001)
3. P. S. Bulson, *The stability of flat plates* (Chatto&Windus, London, 1970)
4. J. Ravinger, M. Psotny, *Structural Analysis. Nonlinear Problems* (ES STU, Bratislava, 2007, in Slovak)
5. J. Ravinger, *Thin. Wall. Struct.* **19**, 1 (1994)
6. D. W. Murray, E. L. Wilson, *AIAA J.*, **7** (1969)
7. J. L. Batoz, G. Dhatt, *Int. J. Numer. Meth. Eng.* **14** (1979)
8. Z. P. Bazant, L. Cedolin, *Stability of Structures - Elastic, Inelastic, Fracture and Damage Theories* (Oxford University Press, New York, Oxford, 1991)
9. J. Havran, M. Psotny, *Applied Mechanics and Materials* **837** (2016)
10. E. Riks, *J. Appl. Mech.* **39** (1972)
11. M. Psotny, J. Ravinger, *Engineering Mechanics* **14**, 6 (2007)
12. I. Veghova, M. Psotny, *MATEC Web of Conferences* **310**, 00018 (2020)
13. M. Psotny, *AIP Conference Proceedings* **1863**, 260007 (2017)
14. ANSYS User's Manual 13.0. Swanson Analysis Systems, Inc. (2010)